



Comparison of water use efficiency and biomass production in 10-year-old *Populus sibirica* and *Ulmus pumila* plantations in Lun soum, Mongolia

Sungsik Cho, Byambadorj Ser-Oddamba, Nyam-Osor Batkhuu & Hyun Seok Kim

To cite this article: Sungsik Cho, Byambadorj Ser-Oddamba, Nyam-Osor Batkhuu & Hyun Seok Kim (2019): Comparison of water use efficiency and biomass production in 10-year-old *Populus sibirica* and *Ulmus pumila* plantations in Lun soum, Mongolia, Forest Science and Technology, DOI: [10.1080/21580103.2019.1634646](https://doi.org/10.1080/21580103.2019.1634646)

To link to this article: <https://doi.org/10.1080/21580103.2019.1634646>



© 2019 The Author(s). Published by Informa UK Limited, trading as Taylor & Francis Group.



Published online: 04 Jul 2019.



Submit your article to this journal [↗](#)



View Crossmark data [↗](#)

Comparison of water use efficiency and biomass production in 10-year-old *Populus sibirica* and *Ulmus pumila* plantations in Lun soum, Mongolia

Sungsik Cho^{a,b}, Byambadorj Ser-Oddamba^c, Nyam-Osor Batkhuu^d and Hyun Seok Kim^{a,b,e,f}

^aInterdisciplinary Program in Agricultural and Forest Meteorology, Seoul National University, Seoul, Republic of Korea; ^bNational Center for Agro Meteorology, Seoul, Republic of Korea; ^cDepartment of Environment & Forest Resources, College of Agriculture and Life Science, Chungnam National University, Daejeon, Republic of Korea; ^dDepartment of Environmental and Forest Engineering, School of Engineering and Applied Sciences, National University of Mongolia, Ulaanbaatar, Mongolia; ^eDepartment of Forest Sciences, Seoul National University, Seoul, Republic of Korea; ^fResearch Institute for Agriculture and Life Sciences, Seoul National University, Seoul, Republic of Korea

ABSTRACT

Although afforestation is one of the best solutions for combating desertification, it requires intensive management. To minimize management efforts in plantations in arid area, it is crucial to select suitable tree species, i.e. those with a high adaptability to xeric environments. In this study, we investigated key tree traits related to drought adaptation in *Populus sibirica* Hort. ex Tausch and *Ulmus pumila* L., planted in the Korea-Mongolia Green Belt Plantation in Lun soum, Mongolia. We found that *U. pumila* had a smaller leaf size and smaller specific leaf area (SLA) than *P. sibirica*. In addition, the water use efficiency (WUE) of *U. pumila* (carbon isotope-based) was significantly higher than that of *P. sibirica*. Although biomass production was ~2.5 times higher in *P. sibirica* than in *U. pumila* due to the differences in leaf area, there were no statistically significant differences in the photosynthetic characteristics on an area basis. These results indicate that *U. pumila* has a higher adaptive potential to dry conditions than *P. sibirica* due to its small leaf size, low SLA, and high WUE.

ARTICLE HISTORY

Received 29 January 2019
Accepted 18 June 2019

KEYWORDS

Photosynthetic characteristics; carbon isotope; biomass production; water use efficiency; reforestation

Introduction

The most common methods for combatting desertification are afforestation and reforestation (Miao et al. 2015; Yan et al. 2015; Fan et al. 2016). However, many afforestation and reforestation efforts, especially large-scale efforts, have been unsuccessful (Choi 2004; Cao 2008; Wang et al. 2010). In addition, improper afforestation can induce unwanted environmental problems (e.g. increased water consumption that may lower the ground water table, reduce water yield, and diminish soil moisture) (Yi and Wang 2013; Cao et al. 2016; Lu et al. 2018). These issues are mainly caused by lack of clear objectives, inadequate management practices, and species selection (Cao S et al. 2011; Cao et al. 2014; Qu et al. 2014). Appropriate species selection is key to the success of afforestation efforts and is especially important for the sustainability of the plantation, which requires long-term monitoring (Cao et al. 2009; Jacobs et al. 2015; Lu et al. 2018). Afforestation species are frequently selected based on their growth capacity, i.e. for fast establishment and quick recovery of degraded areas (Padilla et al. 2009; Zhang et al. 2016). However, although these fast-growing tree species generally grow well at first, some are not able to maintain their fast growth as soil water is depleted and when their water use exceeds the supply of the environment (Cao SX et al. 2011). To avoid these problems, there has been

an increased interest in and use of slow-growing species that are less water-demanding in the afforestation or restoration of desert areas (Liang et al. 2006; Chazdon 2008; Padilla et al. 2009; Cao S et al. 2011; Jacobs et al. 2015; Lu et al. 2018).

For successful restoration, it is necessary to consider whether the planted trees have species-specific adaptive strategies to drought-stressed environments. For instance, xeromorphic traits, such as the small leaf size or specific leaf area (SLA, or its reciprocal, leaf mass per area) can help overcome extremely dry conditions (Haworth and McElwain 2008). In addition to morphological traits, changes in plant stomatal conductance (g_s) are considered the main physiological mechanisms to regulate leaf transpiration-induced leaf water deficit (Farquhar and Sharkey 1982) and to avoid irreversible damage in the plant hydraulic system (Chaves 1991; Medrano 2002; Pivovarov et al. 2016). Eventually, the reduction in g_s in a prolonged water-stressed condition leads to a decrease in photosynthesis (Chaves 1991). Interestingly, however, certain biochemical property in the leaves can improve photosynthetic capacity at given values of g_s by partially compensating the reduction of photosynthesis due to the stomatal limitation (Wright et al. 2001; Hinojo-Hinojo et al. 2018). These key measurements of photosynthetic capacity include the rate parameters: the

maximum rate of carboxylation (V_{Cmax}) and maximum rate of electron transport (J_{max}) (Farquhar et al. 1980; Wullschlegel 1993). Thus, the improvement of these photosynthetic properties could increase the intrinsic water use efficiency (WUE_i), which is estimated as the ratio between maximum photosynthetic rate (A_{max}) at g_s , even though the g_s reduces access to CO_2 when the plants are drought stressed (Medrano et al. 2009).

Especially in water-limited environments, plants should minimize water loss while maximizing carbon uptake to optimize their water-use strategies (e.g. Galiano et al., 2011; Adams et al., 2013; Mitchell et al., 2013). For this reason, water use efficiency (WUE) is an important indicator of plant adaptability and sustainability, especially under drought stress. The relationship between WUE and drought tolerance is, however, more difficult to establish and thus to use in the selection of species for afforestation or reforestation efforts in arid regions. Some researchers have proposed that drought-tolerant species with high WUEs are more beneficial than fast-growing species with lower WUEs under water-limited conditions (Fischer and Turner, 1978; Ehleringer and Cooper, 1988). In contrast, other researchers have argued that drought-tolerant species should have low WUEs because they have conservative morphological and physiological strategies that results in low photosynthetic rates than those of species with high WUEs (Delucia and Schlesinger, 1991; Miller et al., 2001). Consequently, for sustainable conservation, it is necessary to understand the various responses, mechanisms, and strategies underpinning tree species, especially those used (or may potentially be used) for afforestation and reforestation.

Populus sibirica Hort. ex Tausch and *Ulmus pumila* L. are the two most commonly planted species used to combat desertification (i.e. used in afforestation or restoration efforts) in Mongolia (Jo and Park 2017). *Populus sibirica* is widely used for its high productivity, re-sprouting capability, and easy vegetative propagation, but it requires a relatively higher water supply due to its rapid growth (Rhodenbaugh and Pallardy 1993; Isebrands and Richardson 2014). On the other hand, *U. pumila* is considered to have high drought resistance due to its natural existence in the Mongolian desert, but it shows slow growth (Hilbig 1995). Despite their frequent use as restoration species, *P. sibirica* has not been well studied after its introduction from Russia in the 1940s; and similarly, *U. pumila* has been reported in only a few studies conducted in the forest steppes of Mongolia (Dulamsuren et al. 2005a, 2005b; Dulamsuren et al. 2009). In this study, we compared two common afforestation species, *P. sibirica* and *U. pumila*, planted in the Korea-Mongolia Green Belt Plantation in Lun soum, Mongolia, in 2008. We tested the following hypotheses: (1) the leaf morphology (leaf size and SLA) of the fast-growing *P. sibirica* is larger than that of *U. pumila* and demonstrates less seasonal variation; (2) under drought stress, *P. sibirica* accumulates more biomass by maintaining a higher g_s and A_{max} ; and (3) the WUE of

U. pumila is higher than that of *P. sibirica*. We tested these hypotheses by comparing the morphological and physiological differences, stomatal regulation behavior, WUE_i , and the discrimination of the C isotope ($\Delta^{13}C$) of these species. Leaf size and SLA were used to investigate the morphological characteristics and the A_{max} , V_{Cmax} , and J_{max} photosynthetic traits were used to investigate the physiological characteristics. To test the physiological adaptations to drought conditions, we compared the WUE_i and $\Delta^{13}C$. Finally, we assessed how the species-specific strategies related to the aboveground biomass (AGB) increments by estimating the growth of *P. sibirica* and *U. pumila* during the growing season.

Materials and methods

Site description

The study site was located at the Korea-Mongolia plantation in Lun soum, Tov aimag; 135 km west of Ulaanbaatar, Mongolia (Figure 1). It is located at 47°51'27.1"N, 105°8'51"E, with an elevation of 1130 m. The area is in a semi-arid region, with an average temperature of 0.6 ± 0.45 °C, a growing season temperature of 16.29 ± 0.41 °C (May–September), and an average annual precipitation of 206.62 ± 22.45 mm from 1989 to 2013 in Lun station, Mongolia (NAMEM, 2013). Summer precipitation occurs between June and August, and accounts for 80–90% of the total annual rainfall. The mean annual potential evapotranspiration was 752.12 ± 30.68 mm; during the growing season of the Mongolian Plateau grassland from 1981 to 2013, it was 565.38 ± 26.94 mm (Cao et al. 2018).

Study plots and growth measurements

The study plots were located inside the plantation, in a 50 ha area (1000 m × 500 m). The trees were planted within a 20.88 ha area and the rest of area was left for agroforest use. Three-year-old *P. sibirica* and *U. pumila* (total $n = 27,348$ trees), were planted in alternating lines in 2008. The distance between rows and the planting distance between trees were 4 m and 2 m, respectively (Figure 1). Trees were subjected to one of two irrigation regimes: 2 L (= 0.25 mm m^{-2}) per hour and 4 L (= 0.5 mm m^{-2}) per hour. Irrigation was performed once every 6 days, from mid-May until September 2014 (total $n = 30$ irrigation events), the last of which occurred on September 28. The duration of irrigation was 6 hours, during which time 2 L or 4 L water per hour was provided through drip irrigation. Sixteen trees were selected from each species (total $n = 32$ trees), with eight trees selected per irrigation regime for each species.

The diameter and height of trees were measured at the beginning (July 7, 2014) and end (October 27, 2014) of the study period for biomass estimates. Tree diameters were measured twice per tree at 5 cm above the ground surface, in the north-south and east-west directions, using a Vernier caliper (Absolute Digimatic Caliper, Mitutoyo, Kanagawa, Japan; 0.01 mm precision). Tree height was measured using a steel tape.

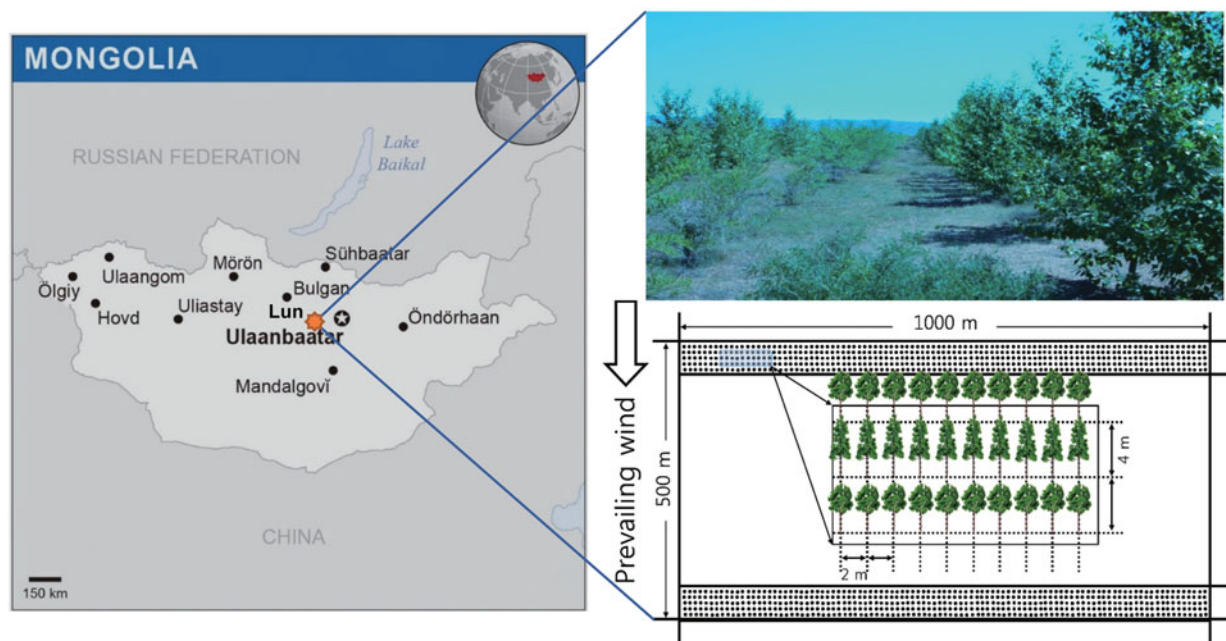


Figure 1. Map location of Lun soum in Mongolia, photograph of study site, and an example of the plantation design used in the study plots. The *Populus sibirica* and *Ulmus pumila* were planted in alternating lines. The distance between rows and the planting distance between trees were 4 m and 2 m, respectively.

Table 1. Tree heights and root collar diameters of sampled *Populus sibirica* and *Ulmus pumila* grown under different irrigation regimes.

Species Treatment	<i>Populus sibirica</i>		<i>Ulmus pumila</i>	
	Irrigation		Irrigation	
Rate ($L h^{-1}$)	2 ($n=8$)	4 ($n=8$)	2 ($n=8$)	4 ($n=8$)
Tree height (m)	4.25 ± 0.40	5.01 ± 0.21	3.34 ± 0.13	2.98 ± 0.48
Diameter at root collar (mm)	74.85 ± 6.76	82.07 ± 5.71	60.38 ± 3.32	47.85 ± 6.29

n = number of trees sampled per treatment. No significant differences were detected for height and root collar diameters of both *P. sibirica* (root collar diameter, $P = 0.345$; height, $P = 0.112$) and *U. pumila* (root collar diameter, $P = 0.107$; height, $P = 0.494$) under different irrigation regimes. Data represent means \pm SE for growth recorded before starting the measurement (SE = standard error).

The heights and diameters for each treatment are listed in Table 1. There was an increasing trend in the tree heights and diameters when the irrigation quantity increased for *P. sibirica*, while those of *U. pumila* showed the opposite trend, i.e. their heights and diameter decreased with increased irrigation. However, no statistical differences in diameter and height growth were detected between the two irrigation regimes for both species (minimum p -value = 0.11). Furthermore, no statistically significant differences were detected in the morphological and physiological traits between irrigation regimes. Therefore, we used the combined data from the two irrigation regimes to increase the statistical confidence and power of the analysis.

Environmental variables

Meteorological data were measured from July to September and included air temperature (T_a ; °C), relative humidity (RH; %), volumetric soil water content (θ ; %), photosynthetically active radiation (Q ; $\mu mol m^{-2} s^{-1}$), and precipitation (mm). The T_a and RH were measured using a HOBO Micro Station (H21-002, Onset Computer Corporation, Cape Cod, MA, USA). Q was measured using a Li-Cor 190 (Campbell Scientific Inc., Logan, UT, USA). The instruments were installed on a 7 m high tower. For data validation and accuracy, we also used T_a , RH (HMP155, Vaisala,

Helsinki, Finland), and precipitation (TE525MM, Texas Electronics, Dallas, TX, USA) data measured at an eddy covariance tower 1500 m away from our study plots. The θ , up to a depth of 30 cm, was measured using a CS616 (Campbell Scientific Inc.). Three sensors were used for each tree species and three additional sensors were installed on bare land to determine the effects of irrigation. All the environmental variables were recorded using a data logger (CR1000, Campbell Scientific Inc.), that collected data at 15 s intervals and recorded after averaging 30 min of data. Due to power loss, Q data were not available from day of year (DOY) 182 to DOY 191 and θ data were not collected from DOY 210 to DOY 221. The error data that were received from several soil moisture sensors were corrected by regression with the data from the other sensors.

Leaf characteristics

To measure leaf size and SLA, leaves from the 32 sampled trees were collected three times: on DOY 207, 221, and 249. In total, 10 to 12 leaves were collected from each sampled tree at various heights, from the south-facing canopy. The leaves were imaged using a scanner (HP Laserjet M1132 MFP, Boise, ID, USA) at 600 dpi resolution and processed by MATLAB (R2014b; Math Works Inc., Natick, MA, USA) to calculate leaf size. Leaf weights were measured to the 0.001 g using a

scale (Discovery Semi-Micro and Analytical Balance, Ohaus Corp., Switzerland), after being dried in a convection oven (OF-11E, Jeio Tech., Republic of Korea) at 65 °C for 3 days. The SLA ($\text{cm}^2 \text{g}^{-1}$) was calculated from the dry leaf weight (g) divided by the leaf size (cm^2).

Photosynthesis measurements and intrinsic water use efficiency (WUE_i)

The rate of photosynthesis was determined using a portable photosynthesis measurement system (LI-6400, Li-Cor Inc., Lincoln, NE, USA), equipped with $2 \times 3 \text{ cm}^2$ red and blue light source chambers (red + blue 6400-02B, Li-Cor Inc.). To measure the light response curve of photosynthesis, the radiation was adjusted from $1500 \mu\text{mol m}^{-2} \text{s}^{-1}$ to $0 \mu\text{mol m}^{-2} \text{s}^{-1}$ in 13 different intensity levels. The sample CO_2 concentration, $[\text{CO}_2]$ in the chamber was controlled at $400 \mu\text{mol mol}^{-1}$ during the measurement. To measure the rate of photosynthesis at various $[\text{CO}_2]$ ($A-C_i$ curve), the $[\text{CO}_2]$ was adjusted from 0 to $1400 \mu\text{mol mol}^{-1}$ in 14 concentration levels. The leaves used for measurements were selected based on locations in the canopy (between 1 m and 2 m, and south-facing), and their similar sizes and quality, and if they were fully unfolded. The leaves were measured after they were stabilized in the chamber environments, which were controlled to maintain a temperature of 25 °C and 55–65% humidity. Six leaves were chosen from the samples of each study species (*P. sibirica* and *U. pumila*) and monitored throughout the study period. The first and second measurements were conducted from DOY 209 to 217, and from DOY 244 to 253, respectively. A_{max} was determined as the value of the photosynthesis reaction curve at $1000 \mu\text{mol m}^{-2} \text{s}^{-1}$. V_{Cmax} and J_{max} were estimated from the acquired CO_2 response curves following Sharkey et al. (2007).

WUE_i ($\mu\text{mol CO}_2 \text{ mol}^{-1} \text{ H}_2\text{O}$), or the quantity of absorbed CO_2 ($\mu\text{mol CO}_2 \text{ m}^{-2} \text{s}^{-1}$) per unit of water consumption ($\text{mol H}_2\text{O m}^{-2} \text{s}^{-1}$), was estimated independently from the leaf gas exchange measurements by using the photosynthetic rate at the light saturation point. WUE_i was calculated as the ratio of A_{max} to g_s .

Stable carbon isotope analyses

To analyze stable carbon isotopes, the 12 leaves per species that were used for the photosynthesis measurements were collected, along with two more leaves from another tree of the same species (total $n = 14$ leaves per species). In addition, a stem core of each sample tree was collected at the end of the growing season using the tree ring core at 5 cm above the root collar, using a 5 mm increment borer (Haglof Sweden AB, Langsele, Sweden). Leaf and stem samples were dried in a convection oven (OF-11E, Jeio Tech.) at 65 °C for 3 days; for the stem sample, the section of the current year was exclusively cut out and used for the analysis. The samples were processed with a homogenizer (FastPrep-24, MP Biomedicals, Solon, OH, USA). The processed specimens were sent to the National Instrumentation Center for Environmental Management (NICEM) at the College of Agriculture

and Life Science, Seoul National University in Korea for the carbon isotope analyses. The composition of the carbon isotopes was analyzed using a mass spectrometer (IsoPrime Vision-EA, Micromass, Manchester, UK) coupled with a CNS analyzer (Elementar group, Hanau, Germany). Carbon isotope ($\delta^{13}\text{C}$) composition was calculated as follows:

$$\delta^{13}\text{C} (\text{‰}) = (R_{\text{sample}}/R_{\text{standard}} - 1) \times 1000 \quad (2)$$

where R_{sample} is the abundance ratio of $^{13}\text{C}/^{12}\text{C}$ in the sample plant, and R_{standard} is the Pee Dee Belemite standard (PDB, 0.0112372‰) for carbon. The accuracy of measurements was assessed using multiple replicated analyses, which indicated that the standard deviation for the $\delta^{13}\text{C}$ measurement was $< 0.1\text{‰}$. The carbon isotope discrimination ($\Delta^{13}\text{C}$) was calculated from the acquired $\delta^{13}\text{C}$ value, following Farquhar et al. (1989).

Aboveground biomass

The aboveground tree biomass (AGB, kg) data were obtained using the allometric equations developed from harvested branches. Five trees of *P. sibirica* and *U. pumila* were sampled from near the experimental site when the leaf area of each species had reached its maximum. Branches ($n = 10\text{--}15$) were collected evenly from throughout the crown each individual tree, which resulted in a total of 98 and 102 branches for *P. sibirica* and *U. pumila*, respectively. The sample collection progressed from the lower to the upper branches to ensure that the size of the branches was the evenly distributed over the entire tree. Branch diameter (measured at 1 cm from point of insertion in the north-south and east-west directions, and twice in each direction), length, and its height (position) on the tree were recorded. After harvested branches were transported to the lab, the leaves were separated from the branches and dried in a convection oven (OF-11E, Jeio Tech.) at 65 °C for 3 days. After drying, the dry weight of the leaves and branches were measured to 0.001 g (Discovery Semi-Micro and Analytical Balance, Ohaus Corp.). Allometric equations for branch diameter and the respective leaf biomass were developed for each species. We tested some power equations (with the diameters of the studied trees) using the most reliable models, based on R^2 , and scaled them up from the sample trees to all trees. Stem biomass (SB) was calculated using the cylinder formula. Stem volume was converted to dry weight using the equation:

$$\text{SB} = \pi \times (\text{DRC}/2)^2 \times \text{tree height}/3 \times \text{DEN} \quad (3)$$

where DRC and DEN denote the diameter root collar and the wood density, respectively. Finally, AGB was calculated as the sum of SB, total branch, and leaf biomass of each measured tree. Allometric equations for AGB were developed using simple linear regression with DRC as the independent variable (Rawat and Singh 1988). The allometric equations used were:

$$\text{AGB}_{P.sibirica} = 171.19 \times \text{DRC} - 7808.4 \quad (R^2 = 0.92) \quad (4)$$

$$AGB_{U.pumila} = 90.159 \times DRC - 1641.4 \quad (R^2 = 0.98) \quad (5)$$

Data analysis

Student's *t*-tests were used to compare the means after data were tested for normality (Shapiro-Wilk test) and homogeneity of variance (Levene's test). If the data did not satisfy the normality and homogeneity tests, Mann-Whitney tests were used to compare the differences. The statistical analyses were conducted in SPSS 22.0 (IBM Corp., SPSS Statistics for Windows, Chicago, IL, USA). Data were presented as means \pm standard errors (SEs). *p*-Values < 0.05 were considered statistically significant. We compared SLA, A_{max} , V_{Cmax} , J_{max} , WUE_i , and $\Delta^{13}C$ using analysis of variance (ANOVA) and Tukey's standardized multiple comparisons test to identify significant differences among groups (Norusis 2008). We compared the linear regression lines for the relationships between V_{Cmax} and J_{max} , g_s and WUE_i , A_{max} and WUE_i , and $\Delta^{13}C$ for the two species using analysis of covariance (ANCOVA), after analyzing the regressions to elucidate significant differences between the two species. Soil moisture was evaluated using a Kruskal-Wallis nonparametric test. The graphs were

produced using Sigma Plot version 12.5 (Systat Software for windows, San Jose, CA, USA).

Results

Environmental variables

The meteorological data during the period of DOY 182 to DOY 263 showed that the average and highest T_a of Lun soum were 17.31 and 33.66 °C, respectively (Figure 2a). The T_a followed the change of the seasons, peaking at mid-July to early August and decreasing in September. The mean daily *D* and *Q* were 1.08 kPa, and 534.08 $\mu\text{mol m}^{-2} \text{s}^{-1}$, respectively (Figures 2b, c). The total precipitation during the study period was 109.8 mm, where 71.6 mm, 8.6 mm, and 29.6 mm, were recorded in July, August, and September, respectively (Figure 2d). *D* peaked in August due to little precipitation and high T_a . *Q* was highest in July, probably due to the missing data in June. θ showed a higher value in July and September than in August, due to the precipitation (Figure 2e). The average θ of the *U. pumila* plot was $9.88 \pm 0.23\%$, which was higher than that of the *P. sibirica* plot ($9.03 \pm 0.23\%$). θ was higher in the treatment plots than in the control plot ($7.28 \pm 0.27\%$), due to the irrigation showing clear enhancement of θ after irrigation ($p < 0.001$, Figure 2e).

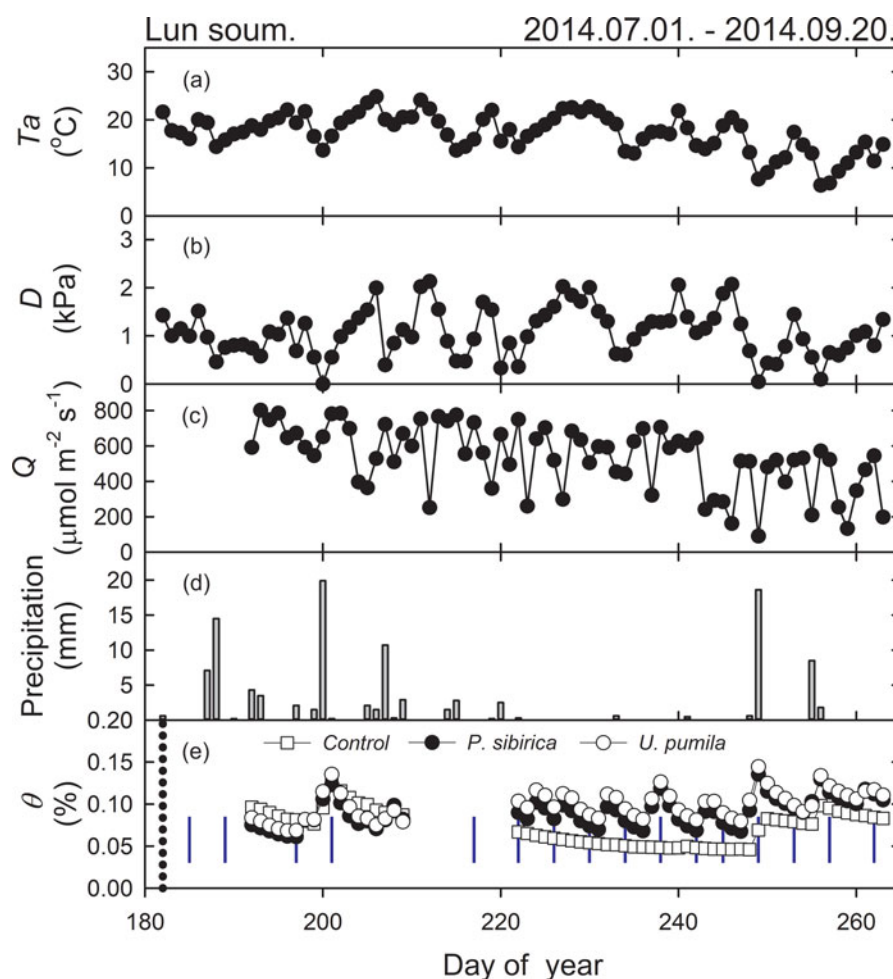


Figure 2. Daily average environmental variables in Lun soum plantation (a) Average daily mean temperature (T_a , °C), (b) vapor pressure deficit (*D*, kPa), (c) photosynthetically active radiation (*Q*, $\mu\text{mol m}^{-2} \text{s}^{-1}$), (d) precipitation (mm), and (e) soil volumetric water content (θ , %) measured at the study site between July and September 2014. (□) Control, (●) *Populus sibirica*, (○) *Ulmus pumila*; (|), blue vertical line, represents irrigation treatment.

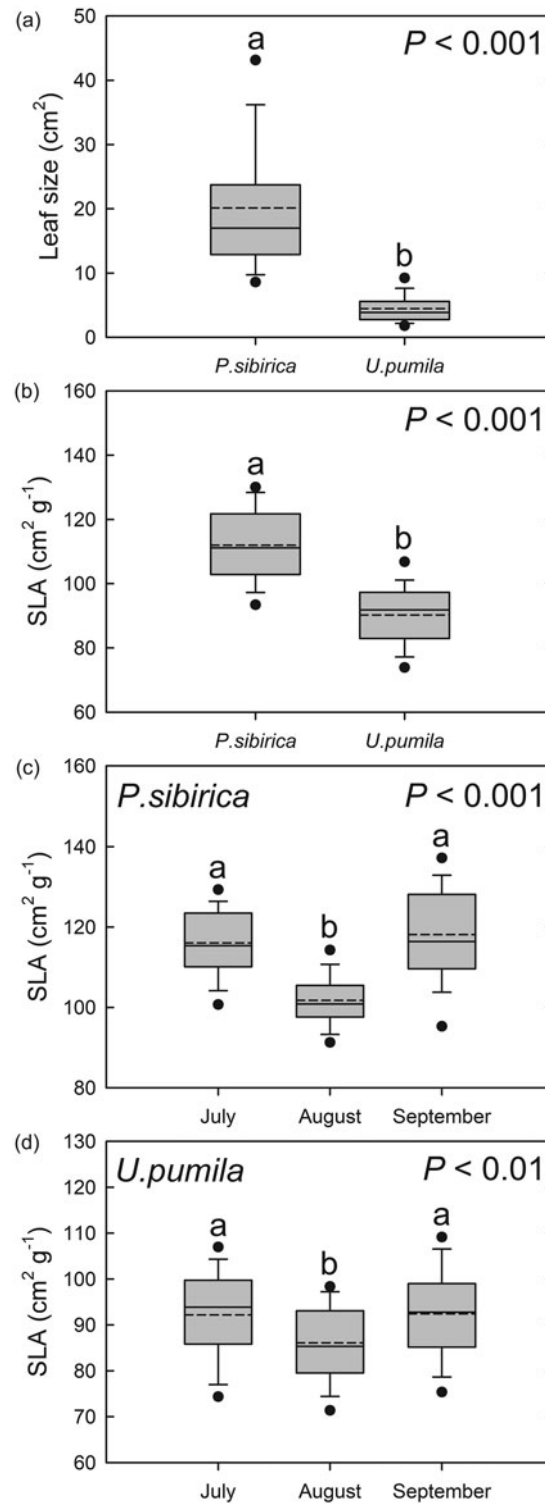


Figure 3. Comparisons of average leaf size (cm²) and specific leaf area (SLA, cm² g⁻¹) of *Populus sibirica* and *Ulmus pumila*. (a) Interspecies comparison of leaf size ($p < 0.001$), (b) interspecies comparison of SLA ($p < 0.001$), (c) seasonal changes in the SLA of *P. sibirica* ($p < 0.001$), and (d) seasonal changes in the SLA of *U. pumila* ($p < 0.01$). Contained within each box are the lower quartile, median (dash), mean (short dash), and upper quartile of the values. Different letters on the error bars indicate significant differences according to the t -test and Tukey's multiple range test at $p < 0.05$.

Morphological characterization of the leaves

The average leaf size of *P. sibirica* was larger than that of *U. pumila*. ($p < 0.001$, Figure 3a). Similarly, the average SLA of *P. sibirica* was also larger than that of *U. pumila*. ($p < 0.001$, Figure 3b). There were significant variations with seasonal change in SLA within species for both species: the SLA of *P. sibirica* was 116.07 ± 1.49 , 101.73 ± 1.13 , and 118.13 ± 2.08 cm² g⁻¹ in July, August, and September, respectively, and that of *U. pumila* was

92.19 ± 1.64 , 86.09 ± 1.44 , and 92.44 ± 1.70 cm² g⁻¹, respectively (Figures 3c, d). Both species had smaller SLAs in August than in July and September ($p < 0.001$, $p < 0.01$ for *P. sibirica* and *U. pumila*, respectively).

Estimation of A_{max} photosynthesis parameters

A_{max} of *P. sibirica* was affected by seasonal change, showing a higher value in August and a decrease in

September ($p < 0.001$, Figure 4a). A_{\max} of *U. pumila*, however, did not show such changes, and was 23.18 ± 1.32 and $20.35 \pm 2.03 \mu\text{mol CO}_2 \text{ m}^{-2} \text{ s}^{-1}$ in August and September, respectively ($p = 0.266$, Figure 4a). In August and September, A_{\max} did not differ between *P. sibirica* and *U. pumila* ($p = 0.242$ and $p = 0.154$, respectively, Figure 4a). V_{Cmax} and J_{max} were higher in August than in September for both species ($p < 0.001$ and $p < 0.01$, Figures 5b and c, respectively). In August and September, V_{Cmax} and J_{max} did not differ between *P. sibirica* and *U. pumila*.

The relationship between V_{Cmax} and J_{max} was not significantly different between species (ANCOVA analysis, $p = 0.819$). The overall means of V_{Cmax} and J_{max} were 122.16 ± 5.31 and $158.16 \pm 5.14 \mu\text{mol m}^{-2} \text{ s}^{-1}$, respectively, and both parameters were linearly correlated. As a result, the linear regression equation for the two species is given as (Figure 4d):

$$J_{\max} = 0.83 \times V_{\text{Cmax}} + 56.27 \quad (R^2 = 0.74, p < 0.001)$$

The relationship between WUE_i , g_s , and A_{\max} across species

Differences in WUE_i were seasonally dependent. In August, the WUE_i of *U. pumila*, was higher than that

of *P. sibirica* ($p < 0.01$). In September, however, there was no difference between the WUE_i of *U. pumila* and *P. sibirica* ($p = 0.095$). Within species, the WUE_i of *P. sibirica* differed between August and September ($p < 0.01$), while that of *U. pumila* did not ($p = 0.072$, Table 2).

A strong negative, but non-linear relationship was found between g_s and WUE_i (Figure 5a). WUE_i decreased as g_s increased in both species (Figure 5a). The relationship between g_s and WUE_i of *P. sibirica* was more robust ($R^2 = 0.96$) and had broader ranges of g_s ($0.04\text{--}0.54 \text{ mol m}^{-2} \text{ s}^{-1}$) than *U. pumila* ($R^2 = 0.61$ and $0.02\text{--}0.38 \text{ mol m}^{-2} \text{ s}^{-1}$, respectively). However, the relationships between WUE_i and g_s for both species did not differ significantly (overall $\text{WUE}_i = (0.19 \times 0.20)/(0.20 + g_s)$, $R^2 = 0.80$, $p < 0.001$, Figure 5a). The relationship between A_{\max} and WUE_i showed a negative correlation: WUE_i decreased as A_{\max} increased in both species (Figure 5b). Similar to g_s , a stronger negative linear relationship was found in *P. sibirica* ($\text{WUE}_i = -0.006 \times A_{\max} + 0.204$, $R^2 = 0.84$, $p < 0.001$) than in *U. pumila* ($\text{WUE}_i = -0.002 \times A_{\max} + 0.153$, $R^2 = 0.17$, $p < 0.05$). In addition, the slope of the relationship between A_{\max} and WUE_i of *P. sibirica* was steeper than that of *U. pumila* ($p < 0.01$, Figure 5b).

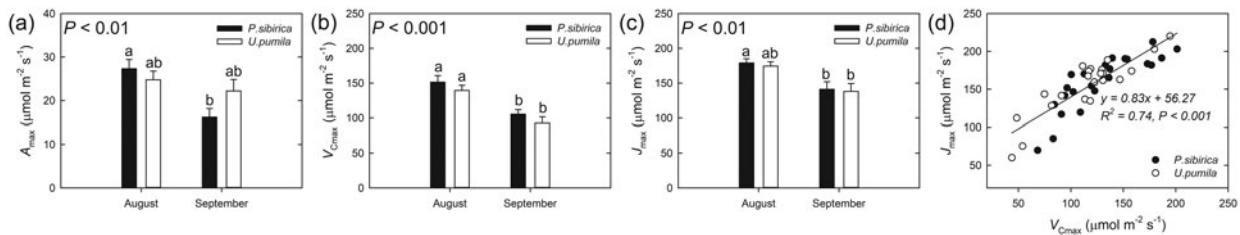


Figure 4. Comparisons of photosynthetic characteristics between *Populus sibirica* and *Ulmus pumila*. (a) Seasonal differences in the maximum rates of photosynthesis (A_{\max} , $\mu\text{mol m}^{-2} \text{ s}^{-1}$) of *P. sibirica* and *U. pumila* ($p < 0.01$), (b) seasonal differences in the maximum rate of carboxylation (V_{Cmax} , $\mu\text{mol m}^{-2} \text{ s}^{-1}$) of *P. sibirica* and *U. pumila* ($p < 0.001$), (c) comparison of the maximum rate of electron transport (J_{\max} , $\mu\text{mol m}^{-2} \text{ s}^{-1}$) of *P. sibirica* and *U. pumila* ($p < 0.01$), and (d) the relationship between V_{Cmax} and J_{\max} . Closed circles (●) and open circles (○) represent *P. sibirica* and *U. pumila*, respectively. The solid line represents the regression line ($J_{\max} = 0.83 \times V_{\text{Cmax}} + 56.27$, $R^2 = 0.74$, $p < 0.001$). Different letters on the error bars indicate significant differences according to *t*-test and Tukey's multiple range tests at $p < 0.05$. The differences in the regression were calculated using analysis of covariance (ANCOVA).

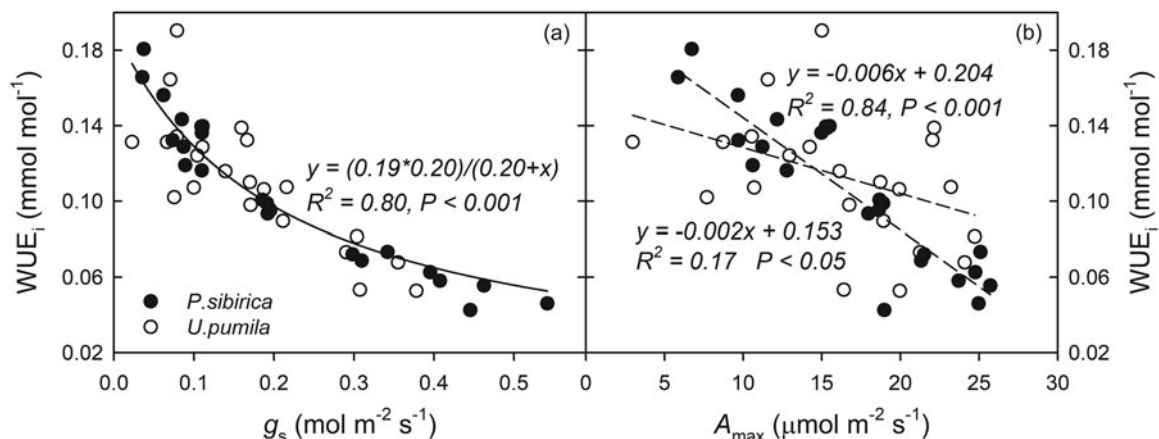


Figure 5. Comparisons of the intrinsic water use efficiency (WUE_i), stomatal conductance (g_s), and maximum photosynthetic capacity (A_{\max}) between *Populus sibirica* and *Ulmus pumila*. (a) The relationship between g_s ($\text{mol m}^{-2} \text{ s}^{-1}$) and WUE_i (mmol mol^{-1}) in *P. sibirica* and *U. pumila*. The curve is a non-linear regression line fit to all data. (b) The relationship between A_{\max} ($\mu\text{mol m}^{-2} \text{ s}^{-1}$) and WUE_i in *P. sibirica* and *U. pumila*. The dashed lines are linear regression through the data points for the two individual species. Closed circles (●) and open circles (○) represent *P. sibirica* and *U. pumila*, respectively.

Table 2. Intrinsic water use efficiency (WUE_i, mean ± SE) of *Populus sibirica* and *Ulmus pumila* over two months.

Species Month	<i>Populus sibirica</i>		<i>Ulmus pumila</i>	
	August	September	August	September
WUE _i (μmol CO ₂ mol ⁻¹ H ₂ O)	83.81 ± 8.96 ^b	128.03 ± 12.25 ^a	125.48 ± 9.14 ^a	101.15 ± 9.05 ^{ab}

Different superscript letters indicate significant differences between months ($P < 0.01$) at the 5% level.

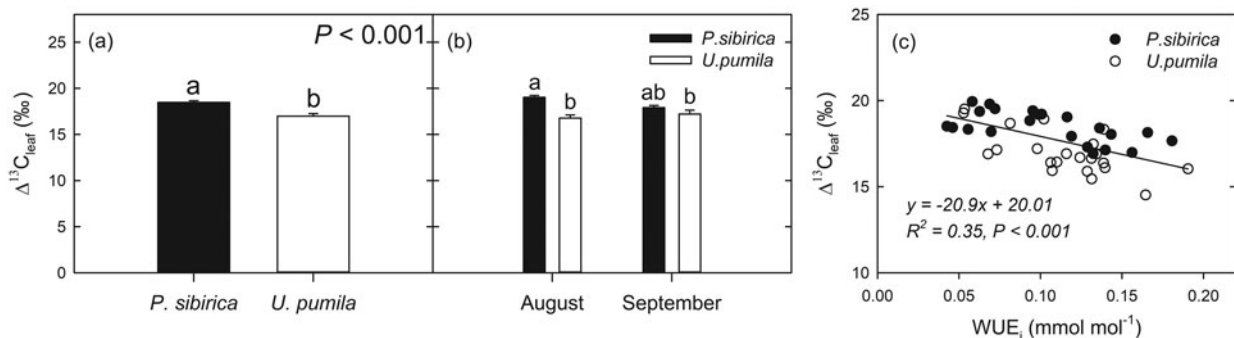


Figure 6. Comparisons of the carbon isotope discrimination ($\Delta^{13}C$) and WUE_i between *Populus sibirica* and *Ulmus pumila*. (a) Values of $\Delta^{13}C$ (‰, mean ± SE) calculated from carbon isotope composition ($\delta^{13}C$) for *P. sibirica* and *U. pumila*. (b) Mean values of $\Delta^{13}C$ over the 2 months, respectively. Different lowercase letters above the error bars indicate significant differences at $p < 0.05$. (c) Relationships between $\Delta^{13}C$ and intrinsic water use efficiency (WUE_i, mmol mol⁻¹) for *P. sibirica* and *U. pumila*. The solid line represents the linear regression through the data points for both species.

Carbon isotope discrimination and intrinsic water use efficiency (WUE_i) of leaves

The $\Delta^{13}C$ of *U. pumila* was lower than that of *P. sibirica* ($p < 0.001$, Figure 6a). Seasonal changes in $\Delta^{13}C$ in *P. sibirica* were observed: 19.03 ± 0.2 and 17.91 ± 0.24 ‰ in August and September, respectively ($p < 0.01$, Figure 6b), but not in *U. pumila*: 16.77 ± 0.35 and 17.21 ± 0.42 ‰ in August and September, respectively ($P = 0.433$, Figure 6b). The relationship between $\Delta^{13}C$ and WUE_i showed a negative correlation, and there was no difference between species ($\Delta^{13}C = -20.9 \times \text{WUE}_i + 21.01$, $R^2 = 0.35$, $p < 0.001$, Figure 6c).

Aboveground biomass growth and carbon isotope discrimination of stems

Aboveground biomass (AGB) of *P. sibirica* and *U. pumila* changed from 5.71 ± 0.74 and 3.26 ± 0.35 kg tree⁻¹ in the pre-measurement to 6.31 ± 0.74 and 3.57 ± 0.35 kg tree⁻¹ in the post-measurement, respectively (Figure 7a). Net AGB production was significantly different between *P. sibirica* and *U. pumila*, i.e. 0.6 ± 0.06 and 0.31 ± 0.03 kg tree⁻¹, respectively ($p < 0.001$, Figure 7a). Leaf area production also differed significantly between *P. sibirica* and *U. pumila*: 13.66 ± 2.36 and 7.43 ± 0.86 m² tree⁻¹, respectively ($p < 0.05$, Figure 7b). The $\Delta^{13}C_{\text{stem}}$ of *U. pumila* (17.64 ± 0.27 ‰) was significantly lower than that of *P. sibirica* (18.72 ± 0.18 ‰) ($p < 0.01$, Figure 7c).

Discussion

Morphological differences in leaf size and SLA

Ulmus pumila was found to have smaller and thicker leaves (smaller SLA) than *P. sibirica*. The low SLA recorded for *U. pumila* would enable reduced water loss, a thick cuticle layer, and deeply sunken stomata

(Figures 3a, b) (Givnish 1987; Park et al. 2016; Leigh et al. 2017). In addition, the small leaves of *U. pumila* might result in the species being less stressed and better adapted to heat stress by preventing heat accumulation due to efficient coupling of leaves with the surrounding environment (Gibson 1998; Monteith and Unsworth 2013; Leigh et al. 2017). These findings are further corroborated by the fact that *U. pumila* is naturally found in arid regions (Wesche et al. 2011).

The SLAs of *P. sibirica* and *U. pumila* were dependent on seasonal changes, and were lower in August than in July and September due to low precipitation and high temperatures (Coble et al. 2016; Fajardo and Siefert 2016). Furthermore, the trees in our study area consisted of two evenly distributed young species, which seemed to induce a higher soil moisture loss rate due to the increased transpiration than when planted as a single species (Delzon and Loustau 2005). Similar results have often been reported for seasonal changes in SLA and other leaf traits caused by water stress in hardwood species (e.g. Wilson et al. 2000; Xu L and Baldocchi 2003; Nouvellon et al. 2010; Chen et al. 2015). In addition, Gotsch et al. (2010) showed that leaf characteristics are more relevant in dry than in wet conditions.

However, the SLA of both species increased in September, but the reasons for this change seem to differ between species. The larger SLA in *P. sibirica* may be due to nutrient reallocation for the upcoming senescence that resulted in a lighter and the larger SLA (Jurik 1986; Han et al. 2008). *Populus sibirica* showed higher seasonal variation than *U. pumila*, which showed no changes in A_{max} between August and September (Figure 4a). A rapid reduction in photosynthetic rate, which is characteristic of senescing leaves, appears to have occurred during the late autumn season (Herrick and Thomas 2003; Katahata et al. 2007). In addition, *P. sibirica*, being a fast-growing species with higher photosynthetic capacity, generated larger and thinner leaves with a shorter leaf longevity

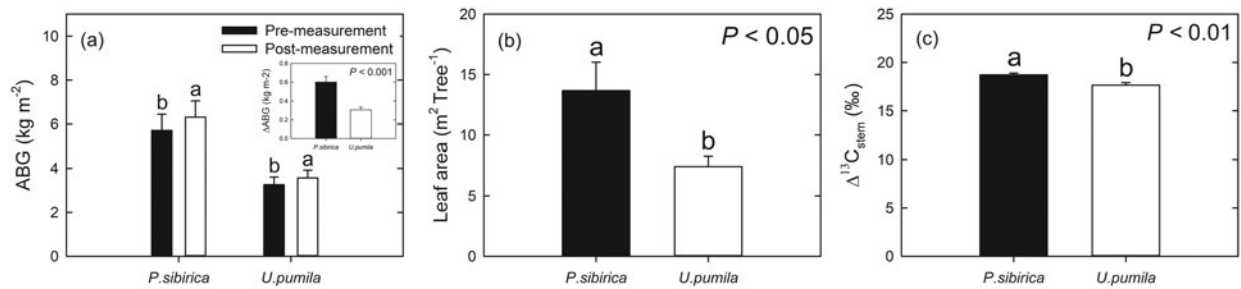


Figure 7. (a) Mean values of aboveground biomass (ABG, kg m⁻²) for *Populus sibirica* and *Ulmus pumila*. The inset presents the changes in ABG between pre-measurement and post-measurement. (b) Leaf area (m² tree⁻¹) of *P. sibirica* and *U. pumila*. (c) The values of stem carbon isotope discrimination (‰ $\Delta^{13}\text{C}$, mean \pm SE) calculated from the carbon isotope compositions ($\delta^{13}\text{C}$) of *P. sibirica* and *U. pumila*. Different lowercase letters above the error bars indicate significant differences at $p < 0.05$.

than the smaller, longer-lived leaves of *U. pumila* (Reich et al. 1997; Reich et al. 1999). These results suggest that variations in SLA can be attributed to seasonal changes in the re-translocation processes of leaf nutrients or non-structural carbohydrate contents (Misson et al. 2006).

Differences in photosynthesis parameters

Mongolia is characterized by a long, cold winter, with a very short growing season. Species with short-lived leaves in harsh environments tend to invest more resources in their photosynthesis efficiency rather than their structure (Cunningham et al. 1999; Fonseca et al. 2000; Ackerly et al. 2002). The A_{\max} data ($21.77 \pm 1.22 \mu\text{mol CO}_2 \text{ m}^{-2} \text{ s}^{-1}$) in the present study were surprisingly higher than that of the 5- to 20-year-old *U. pumila* ($15 \mu\text{mol CO}_2 \text{ m}^{-2} \text{ s}^{-1}$) reported from a similar environment in China with an altitude of 1300 m and around 350 mm of precipitation (Su et al. 2014). Similarly, *P. sibirica* had a higher A_{\max} value ($27.31 \pm 2.12 \mu\text{mol CO}_2 \text{ m}^{-2} \text{ s}^{-1}$ in August) than has been reported in warmer and wetter environments (average temperature of 3.7 °C and annual precipitation of 550 mm), i.e. $20.05 \mu\text{mol m}^{-2} \text{ s}^{-1}$ (Xu et al. 2008) (Figure 4a). A high A_{\max} , such as reported by Wright et al. (2001) and Hinojo-Hinojo et al. (2018), is assumed to increase the photosynthetic rate per unit leaf size by improving the biochemical properties such as nitrogen concentration of leaves to overcome low g_s due to moisture stress and a short growing period.

The photosynthetic capacity of a plant is simply expressed with the parameters V_{Cmax} and J_{max} , which represent the enzyme kinetic activity of RuBisCO (ribulose-1,5-bisphosphate carboxylase-oxygenase) and electron transport or ribulose bisphosphate (RuBP) regeneration, respectively (Farquhar et al. 1980). In general, these two parameters have a strong linear relationship ($J_{\text{max}}/V_{\text{Cmax}} = 1.5\text{--}2.0$ at 25 °C; Wullschlegel 1993; Beerling and Quick 1995; Von Caemmerer 2000; Medlyn et al. 2002). However, the $J_{\text{max}}/V_{\text{Cmax}}$ ratio in our study was 0.83 (Figure 4d), which was much lower than the general relationship; this low value was attributed to high V_{Cmax} , rather than low J_{max} . The mean V_{Cmax} in our study was higher than those reported in many empirical studies (Walker et al. 2014; Ali et al. 2015; Nolan et al. 2017). Based on the findings of

other studies, a high V_{Cmax} or low $J_{\text{max}}/V_{\text{Cmax}}$ is common in arid areas, with values ranging from 1.3 to 1.55 (Midgley et al. 2004; Meir et al. 2007; Maseyk et al. 2008; Zhu et al. 2011). The high levels of V_{Cmax} require high RuBisCO activity, which requires a high nitrogen content in the leaves (Reich et al. 1997; Xu L and Baldocchi 2003). The high V_{Cmax} reflects acclimation to abundant irradiance that originates from the high latitude (47°51'27.1"N), altitude (1130 m), and long summer days in Mongolia, because these conditions rarely limit RuBP regeneration. For this reason, trees in arid regions may increase the ability for RuBP carboxylation relatively more than for RuBP regeneration as the best strategy to maintain co-limitation and avoid photo-inhibition as much as possible at high irradiance (Hikosaka et al. 1999).

4.3. Different water-use strategies at various scales

In our study, we examined the water use strategies at three temporospatial scales: intrinsic leaf (i.e. WUE_i), integrated leaf (i.e. $\Delta^{13}\text{C}_{\text{leaf}}$), and integrated biomass (i.e. $\Delta^{13}\text{C}_{\text{stem}}$) (Figures 5, 6, and 7). At the variation in WUE_i across species was not different between species and was primarily driven by variations in g_s (Figure 5a). However, the WUE_i with high A_{\max} was higher in *P. sibirica* than in *U. pumila*, and vice versa with low A_{\max} (Figure 5b). Simply, the short-lived leaves of *P. sibirica* had wider ranges in g_s and WUE_i than the longer-lived leaves of *U. pumila*. These results implied that *U. pumila* controlled g_s more conservatively, maintaining a lower g_s at high A_{\max} than *P. sibirica*. This pattern was consistent at the integrated time scales (Figures 6a and 7c). Significant differences in $\Delta^{13}\text{C}$ between *P. sibirica* and *U. pumila* indicated the different leaf-level time integrated WUE in the two species (Figure 6a). Likewise, the results from stable isotopes in the tree rings of *P. sibirica* and *U. pumila* were significantly different ($p < 0.01$, Figure 7c). The above results offer a good explanation as to why *U. pumila* is distributed throughout the dry desert areas of Mongolia.

Furthermore, *P. sibirica* was found to have higher biomass production than *U. pumila*, presumably by using more water than *U. pumila* (Figures 7a, b). Consistent with this notion, the average soil moisture for *U. pumila* ($9.88 \pm 0.23\%$) was higher than that for *P. sibirica* ($9.03 \pm 0.23\%$) (Figure 2e). The difference in

biomass production is thus presumed to be due to species-specific water consumption and growth characteristics (Ma et al. 2012). *Populus sibirica* has larger leaves and a larger leaf area than *U. pumila*, which also results in the increase in AGB production (Figures 3a and 7b). In addition, Fig. 4a shows that there were no differences in leaf gas exchange per unit leaf area, but Figures 7a, b show the difference in total biomass production due to differences in total leaf area. When the difference in leaf area ($1.84 = 13.66/7.43 \text{ cm}^2 \text{ tree}^{-1}$) was accounted for, the difference in biomass enhancement ($1.96 = 0.6/0.31 \text{ kg tree}^{-1}$) was substantially reduced to $\sim 7\%$ ($1.07 = 1.96/1.84 \text{ kg tree}^{-1}$; Figures 7a, b).

Conclusion

Our study compared the morphological and physiological characteristics as well as the WUE of 10-year-old *P. sibirica* and *U. pumila* trees, i.e. the commonly used species for the afforestation of the Mongolian desert. Regarding the morphological characteristics, *U. pumila*, which is native to and present throughout Mongolia, including the deserts, showed a better adaptation to the desert environment (i.e. small, thick leaves), than did *P. sibirica*, which was introduced from Russia in the mid-twentieth century. In contrast, A_{max} for *P. sibirica*, which is considered to have high productivity, did not differ from that in *U. pumila*, but the biomass yield for *P. sibirica* was nearly double that of *U. pumila*. This difference in biomass production may be attributed to the difference in leaf area and presumably transpiration, as evidenced by the lower soil water content. Even with unfavorable morphological traits for arid areas, *P. sibirica* showed much higher biomass production and had an A_{max} that was more than 1.5 times higher in August than in September. This indicated that *P. sibirica* assimilated a large amount of CO_2 in a short period of time and its physiological activity would be expected to be diminished early. In comparison, the native species *U. pumila* showed small seasonal variations in physiological characteristics, such as A_{max} and J_{max} , and grew slowly over a long period of time. According to the results of this study, *U. pumila* had higher WUE and a consistent A_{max} , while *P. sibirica* exhibited the opposite trends. These findings indicate that *U. pumila* has a lower water requirement than *P. sibirica* in water deficit conditions. Furthermore, *U. pumila* exhibited greater flexibility than did *P. sibirica* in adapting to a dry environment, e.g. Mongolia, via the adoption of a conservative growth strategy. As a result, *P. sibirica* is believed to experience more difficulties in surviving under drought stress conditions, especially due to having such higher water requirements. In addition, the comparison of the morphological and physiological characteristics of the two species revealed that they would have greatly different effects on the water environment and management of plantations, and that *U. pumila* is the more logical choice for use in afforestation efforts in the arid regions of Mongolia.

Acknowledgments

We thank the staff of the Korea-Mongolia Greenbelt Plantation Project and the members of the Forest Genetics and Ecophysiology Laboratory at the National University of Mongolia for their assistance in the laboratory and in the field.

Disclosure statement

No potential conflict of interest was reported by the authors.

Funding

This research was supported by the National Research Foundation of Korea Grant, funded by the Korea Government [grant number NRF-20110032198].

References

- Ackerly D, Knight C, Weiss S, Barton K, Starmer K. 2002. Leaf size, specific leaf area and microhabitat distribution of chaparral woody plants: contrasting patterns in species level and community level analyses. *Oecologia*. 130(3):449–457.
- Adams H D, Germino M J, Breshears D D, Barron-Gafford G A, Guardiola-Claramonte M, Zou C B, Huxman T E. 2013. Nonstructural leaf carbohydrate dynamics of *Pinus edulis* during drought-induced tree mortality reveal role for carbon metabolism in mortality mechanism. *New Phytol.* 197(4): 1142–1151. doi:10.1111/nph.12102.
- Ali AA, Xu C, Rogers A, McDowell NG, Medlyn BE, Fisher RA, Wullschlegel SD, Reich PB, Vrugt JA, Bauerle WL, et al. 2015. Global-scale environmental control of plant photosynthetic capacity. *Ecol Appl.* 25(8):2349–2365.
- Beerling DJ, Quick WP. 1995. A new technique for estimating rates of carboxylation and electron transport in leaves of C_3 plants for use in dynamic global vegetation models. *Global Change Biol.* 1(4):289–294.
- Cao S, Sun G, Zhang Z, Chen L, Feng Q, Fu B, McNulty S, Shankman D, Tang J, Wang Y, et al. 2011. Greening China naturally. *Ambio.* 40(7):828–831.
- Cao S, Zhang J, Chen L, Zhao T. 2016. Ecosystem water imbalances created during ecological restoration by afforestation in China, and lessons for other developing countries. *J Environ Manage.* 183(Pt 3):843–849.
- Cao S. 2008. Why large-scale afforestation efforts in china have failed to solve the desertification problem. *Environ Sci Technol.* 42(6):1826–1831.
- Cao SX, Chen L, Shankman D, Wang CM, Wang XB, Zhang H. 2011. Excessive reliance on afforestation in China's arid and semi-arid regions: lessons in ecological restoration. *Earth-Sci Rev.* 104(4):240–245.
- Cao SX, Chen L, Yu XX. 2009. Impact of China's Grain for Green Project on the landscape of vulnerable arid and semi-arid agricultural regions: a case study in northern Shaanxi Province. *J Appl Ecol.* 46(3):536–543.
- Cao SX, Ma H, Yuan WP, Wang X. 2014. Interaction of ecological and social factors affects vegetation recovery in China. *Biol Conserv.* 180:270–277.
- Cao X-J, Gao Q-Z, Hasbagan G, Liang Y, Li W-H, Hu G-Z. 2018. Influence of climatic factors on variation in the Normalised Difference Vegetation Index in Mongolian Plateau grasslands. *Rangel J.* 40(2):91–100.
- Chaves MM. 1991. Effects of water deficits on carbon assimilation. *J Exp Bot.* 42(234):1–16.
- Chazdon RL. 2008. Beyond deforestation: restoring forests and ecosystem services on degraded lands. *Science.* 320(5882): 1458–1460.
- Chen ZH, Zha TS, Jia X, Wu YJ, Wu B, Zhang YQ, Guo JB, Qin SG, Chen GP, Peltola HL. 2015. Leaf nitrogen is closely

- coupled to phenophases in a desert shrub ecosystem in China. *J Arid Environ.* 122:124–131.
- Choi YD. 2004. Theories for ecological restoration in changing environment: toward 'futuristic' restoration. *Ecol Res.* 19(1): 75–81.
- Coble AP, VanderWall B, Mau A, Cavaleri MA. 2016. How vertical patterns in leaf traits shift seasonally and the implications for modeling canopy photosynthesis in a temperate deciduous forest. *Tree Physiol.* 36(9):1077–1091.
- Cunningham SA, Summerhayes B, Westoby M. 1999. Evolutionary divergences in leaf structure and chemistry, comparing rainfall and soil nutrient gradients. *Ecol Monogr.* 69(4):569–588.
- Delucia, E H, Schlesinger, W H. 1991. Resource-use efficiency and drought tolerance In adjacent great basin and sierran plants. *Ecology.* 72(1):51–58. doi:10.2307/1938901.
- Delzon S, Loustau D. 2005. Age-related decline in stand water use: sap flow and transpiration in a pine forest chronosequence. *Agric Forest Meteorol.* 129(3-4):105–119.
- Dulamsuren C, Hauck M, Mühlenberg M. 2005a. Ground vegetation in the Mongolian taiga forest-steppe ecotone does not offer evidence for the human origin of grasslands. *Appl Vegetat Sci.* 8(2):149–154.
- Dulamsuren C, Hauck M, Mühlenberg M. 2005b. Vegetation at the taiga forest-steppe borderline in the western Khentey Mountains, northern Mongolia. *Ann Bot Fenn.* 42(6): 411–426.
- Dulamsuren C, Hauck M, Nyambayar S, Bader M, Osokhjargal D, Oyungerel S, Leuschner C. 2009. Performance of Siberian elm (*Ulmus pumila*) on steppe slopes of the northern Mongolian mountain taiga: drought stress and herbivory in mature trees. *Environ Exp Bot.* 66(1):18–24.
- Ehleringer, J R, Cooper, T A. 1988. Correlations between carbon isotope ratio and microhabitat in desert plants. *Oecologia.* 76(4):562–566. doi:10.1007/BF00397870.
- Fajardo A, Siefert A. 2016. Phenological variation of leaf functional traits within species. *Oecologia.* 180(4):951–959.
- Fan B, Zhang A, Yang Y, Ma Q, Li X, Zhao C. 2016. Long-term effects of xerophytic shrub *Haloxylon ammodendron* plantations on soil properties and vegetation dynamics in Northwest China. *PLoS One.* 11(12):e0168000.
- Farquhar G, von Caemmerer S, Berry J. 1980. A biochemical model of photosynthetic CO₂ assimilation in leaves of C₃ species. *Planta.* 149(1):78–90.
- Farquhar GD, Ehleringer JR, Hubick KT. 1989. Carbon isotope discrimination and photosynthesis. *Annu Rev Plant Physiol Plant Mol Biol.* 40(1):503–537.
- Farquhar GD, Sharkey TD. 1982. Stomatal conductance and photosynthesis. *Annu Rev Plant Physiol.* 33(1):317–345.
- Fischer, R A, Turner, N C. 1978. Plant productivity in the arid and semiarid zones. *Annu Rev Plant Physiol.* 29(1):277–317. doi:10.1146/annurev.pp.29.060178.001425.
- Fonseca CR, Overton JM, Collins B, Westoby M. 2000. Shifts in trait-combinations along rainfall and phosphorus gradients. *J Ecology.* 88(6):964–977.
- Galiano, L, Martínez-Vilalta, J, Lloret, F. 2011. Carbon reserves and canopy defoliation determine the recovery of Scots pine 4 yr after a drought episode. *New Phytologist.* 190(3): 750–759. doi:10.1111/j.1469-8137.2010.03628.x.
- Gibson AC. 1998. Photosynthetic organs of desert plants. *BioSc.* 48(11):911–920.
- Givnish TJ. 1987. Comparative-studies of leaf form – assessing the relative roles of selective pressures and phylogenetic constraints. *New Phytol.* 106(1):131–160.
- Gotsch SG, Powers JS, Lerda MT. 2010. Leaf traits and water relations of 12 evergreen species in Costa Rican wet and dry forests: patterns of intra-specific variation across forests and seasons. *Plant Ecol.* 211(1):133–146.
- Han QM, Kawasaki T, Nakano T, Chiba Y. 2008. Leaf-age effects on seasonal variability in photosynthetic parameters and its relationships with leaf mass per area and leaf nitrogen concentration within a *Pinus densiflora* crown. *Tree Physiology.* 28(4):551–558.
- Haworth M, McElwain J. 2008. Hot, dry, wet, cold or toxic? Revisiting the ecological significance of leaf and cuticular micromorphology. *Palaeogeogr Palaeoclimatol Palaeoecol.* 262(1-2):79–90.
- Herrick JD, Thomas RB. 2003. Leaf senescence and late-season net photosynthesis of sun and shade leaves of overstory sweetgum (*Liquidambar styraciflua*) grown in elevated and ambient carbon dioxide concentrations. *Tree Physiol.* 23(2): 109–118.
- Hikosaka K, Murakami A, Hirose T. 1999. Balancing carboxylation and regeneration of ribulose-1,5-bisphosphate in leaf photosynthesis: temperature acclimation of an evergreen tree, *Quercus myrsinaefolia*. *Plant Cell Environ.* 22(7):841–849.
- Hilbig W. 1995. The vegetation of Mongolia. Amsterdam: SPB Academic Publishing.
- Hinojo-Hinojo C, Castellanos AE, Llano-Sotelo J, Penuelas J, Vargas R, Romo-Leon JR. 2018. High V_{cmax}, J_{max} and photosynthetic rates of Sonoran Desert species: using nitrogen and specific leaf area traits as predictors in biochemical models. *J Arid Environ.* 156:1–8.
- Isebrands JG, Richardson J. 2014. Poplars and willows: trees for society and the environment. Boston (MA): CABI.
- Jacobs DF, Olliet JA, Aronson J, Bolte A, Bullock JM, Donoso PJ, Landhäuser SM, Madsen P, Peng S, Rey-Benayas JM, et al. 2015. Restoring forests: what constitutes success in the twenty-first century? *New Forests.* 46(5-6):601–614.
- Jo HK, Park HM. 2017. Effects of pit plantings on tree growth in semi-arid environments. *Forest Sci Technol.* 13(2):66–70.
- Jurik TW. 1986. Temporal and spatial patterns of specific leaf weight in successional Northern hardwood tree species. *Am J Bot.* 73(8):1083–1092.
- Katahata SI, Naramoto M, Kakubari Y, Mukai Y. 2007. Seasonal changes in photosynthesis and nitrogen allocation in leaves of different ages in evergreen understory shrub *Daphniphyllum humile*. *Trees-Struct Funct.* 21(6):619–629.
- Leigh A, Sevanto S, Close JD, Nicotra AB. 2017. The influence of leaf size and shape on leaf thermal dynamics: does theory hold up under natural conditions? *Plant Cell Environ.* 40(2): 237–248.
- Liang ZS, Yang JW, Shao HB, Han RL. 2006. Investigation on water consumption characteristics and water use efficiency of poplar under soil water deficits on the Loess Plateau. *Colloids Surf B Biointerfaces.* 53(1):23–28.
- Lu CX, Zhao TY, Shi XL, Cao SX. 2018. Ecological restoration by afforestation may increase groundwater depth and create potentially large ecological and water opportunity costs in arid and semiarid China. *J Cleaner Prod.* 176:1213–1222.
- Ma JX, Chen YN, Li WH, Huang X, Zhu CG, Ma XD. 2012. Sap flow characteristics of four typical species in desert shelter forest and their responses to environmental factors. *Environ Earth Sci.* 67(1):151–160.
- Maseyk KS, Lin T, Rotenberg E, Grunzweig JM, Schwartz A, Yakir D. 2008. Physiology-phenology interactions in a productive semi-arid pine forest. *New Phytol.* 178(3):603–616.
- Medlyn BE, Dreyer E, Ellsworth D, Forstreuter M, Harley PC, Kirschbaum MUF, Le Roux X, Montpied P, Strassmeyer J, Walcroft A, et al. 2002. Temperature response of parameters of a biochemically based model of photosynthesis. II. A review of experimental data. *Plant Cell Environ.* 25(9): 1167–1179.
- Medrano H, Flexas J, Galmes J. 2009. Variability in water use efficiency at the leaf level among Mediterranean plants with different growth forms. *Plant Soil.* 317(1-2):17–29.
- Medrano H. 2002. Regulation of photosynthesis of C₃ plants in response to progressive drought: stomatal conductance as a reference parameter. *Ann Bot.* 89(7):895–905.
- Meir P, Levy PE, Grace J, Jarvis PG. 2007. Photosynthetic parameters from two contrasting woody vegetation types in West Africa. *Plant Ecol.* 192(2):277–287.
- Miao LJ, Moore JC, Zeng FJ, Lei JQ, Ding JL, He B, Cui XF. 2015. Footprint of research in desertification management in China. *Land Degrad Develop.* 26(5):450–457.

- Midgley GF, Araniibar JN, Mantlana KB, Macko S. 2004. Photosynthetic and gas exchange characteristics of dominant woody plants on a moisture gradient in an African savanna. *Global Change Biol.* 10(3):309–317.
- Miller, J M, Williams, R J, Farquhar, G D. 2001. Carbon isotope discrimination by a sequence of Eucalyptus species along a subcontinental rainfall gradient in Australia. *Funct Ecology.* 15(2):222–232. doi:10.1046/j.1365-2435.2001.00508.x.
- Misson L, Tu KP, Boniello RA, Goldstein AH. 2006. Seasonality of photosynthetic parameters in a multi-specific and vertically complex forest ecosystem in the Sierra Nevada of California. *Tree Physiol.* 26(6):729–741.
- Mitchell, P J, O'grady, A P, Tissue, D T, White, D A, Ottenschlaeger, M L, Pinkard, E A. 2013. Drought response strategies define the relative contributions of hydraulic dysfunction and carbohydrate depletion during tree mortality. *New Phytol.* 197(3):862–872. doi:10.1111/nph.12064.
- Monteith J, Unsworth M. 2013. Principles of environmental physics: plants, animals, and the atmosphere. Oxford: Academic Press.
- NAMEM. 2013. The National Agency for Meteorology and Environmental Monitoring of Mongolia. Weather data. <http://namem.gov.mn/eng/?p=56>, accessed September 25.
- Nolan RH, Tarin T, Fairweather KA, Cleverly J, Eamus D. 2017. Variation in photosynthetic traits related to access to water in semiarid Australian woody species. *Funct Plant Biol.* 44(11):1087–1097.
- Norusis M. 2008. SPSS 16.0 guide to data analysis. Upper saddle River (NJ): Prentice Hall Press.
- Nouvellon Y, Laclau JP, Epron D, Kinana A, Mabiala A, Roupsard O, Bonnefond JM, Le Maire G, Marsden C, Bontemps JD, et al. 2010. Within-stand and seasonal variations of specific leaf area in a clonal *Eucalyptus* plantation in the Republic of Congo. *For Ecol Manage.* 259(9):1796–1807.
- Padilla FM, Ortega R, Sanchez J, Pugnaire FI. 2009. Rethinking species selection for restoration of arid shrublands. *Basic Appl Ecol.* 10(7):640–647.
- Park GE, Lee DK, Kim KW, Batkhuu NO, Tsogtbaatar J, Zhu JJ, Jin Y, Park PS, Hyun JO, Kim HS. 2016. Morphological characteristics and water-use efficiency of Siberian Elm Trees (*Ulmus pumila* L.) within arid regions of Northeast Asia. *Forests.* 7(12):280.
- Pivovarov AL, Pasquini SC, De Guzman ME, Alstad KP, Stemke JS, Santiago LS. 2016. Multiple strategies for drought survival among woody plant species. *Funct Ecol.* 30(4):517–526.
- Qu JJ, Cao SX, Li GS, Niu QH, Feng Q. 2014. Conservation of natural and cultural heritage in Dunhuang, China. *Gondwana Res.* 26(3-4):1216–1221.
- Rawat YS, Singh JS. 1988. Structure and function of oak forests in Central Himalaya.1. Dry-matter dynamics. *Ann Bot.* 62(4):397–411.
- Reich, P B, Ellsworth, D S, Walters, M B, Vose, J M, Gresham, C, Volin, J C, Bowman, W D. 1999. Generality of leaf trait relationships: a test across six biomes. *Ecology.* 80(6):1955–1969. doi:10.1890/0012-9658(1999)080[1955:GOLTRA]2.0.CO;2.
- Reich, P B, Walters, M B, Ellsworth, D S. 1997. From tropics to tundra: global convergence in plant functioning. *Proc Natl Acad Sci U S A.* 94(25):13730–13734. doi:10.1073/pnas.94.25.13730.
- Rhodenbaugh EJ, Pallardy SG. 1993. Water stress, photosynthesis and early growth patterns of cuttings of three *Populus* clones. *Tree Physiol.* 13(3):213–226.
- Sharkey TD, Bernacchi CJ, Farquhar GD, Singaas EL. 2007. Fitting photosynthetic carbon dioxide response curves for C₃ leaves. *Plant Cell Environ.* 30(9):1035–1040.
- Su H, Li YG, Liu W, Xu H, Sun OJ. 2014. Changes in water use with growth in *Ulmus pumila* in semiarid sandy land of northern China. *Trees-Struct Function.* 28(1):41–52.
- Von Caemmerer S. 2000. Biochemical models of leaf photosynthesis. Collingwood (Victoria, Australia): Csiro publishing.
- Walker AP, Beckerman AP, Gu L, Kattge J, Cernusak LA, Domingues TF, Scales JC, Wohlfahrt G, Wullschlegler SD, Woodward FI. 2014. The relationship of leaf photosynthetic traits - V_{cmax} and J_{max} - to leaf nitrogen, leaf phosphorus, and specific leaf area: a meta-analysis and modeling study. *Ecol Evol.* 4(16):3218–3235.
- Wang XM, Zhang CX, Hasi E, Dong ZB. 2010. Has the Three Norths Forest Shelterbelt Program solved the desertification and dust storm problems in arid and semiarid China? *J Arid Environ.* 74(1):13–22.
- Wesche K, Walthert D, von Wehrden H, Hensen I. 2011. Trees in the desert: reproduction and genetic structure of fragmented *Ulmus pumila* forests in Mongolian drylands. *Flora.* 206(2):91–99.
- Wilson KB, Baldocchi DD, Hanson PJ. 2000. Spatial and seasonal variability of photosynthetic parameters and their relationship to leaf nitrogen in a deciduous forest. *Tree Physiol.* 20(9):565–578.
- Wright IJ, Reich PB, Westoby M. 2001. Strategy shifts in leaf physiology, structure and nutrient content between species of high- and low-rainfall and high- and low-nutrient habitats. *Funct Ecology.* 15(4):423–434.
- Wullschlegler SD. 1993. Biochemical limitations to carbon assimilation in C₃ plants—a retrospective analysis of the A/Ci Curves from 109 species. *J Exp Bot.* 44(5):907–920.
- Xu L, Baldocchi DD. 2003. Seasonal trends in photosynthetic parameters and stomatal conductance of blue oak (*Quercus douglasii*) under prolonged summer drought and high temperature. *Tree Physiol.* 23(13):865–877.
- Xu X, Peng GQ, Wu CC, Korpelainen H, Li CY. 2008. Drought inhibits photosynthetic capacity more in females than in males of *Populus cathayana*. *Tree Physiol.* 28(11):1751–1759.
- Yan QL, Zhu JJ, Zheng X, Jin CJ. 2015. Causal effects of shelter forests and water factors on desertification control during 2000–2010 at the Horqin Sandy Land region, China. *J for Res.* 26(1):33–45.
- Yi X, Wang L. 2013. Land suitability assessment on a watershed of Loess Plateau using the analytic hierarchy process. *PLoS One.* 8(7):e69498.
- Zhang JG, Lei JQ, Wang YD, Zhao Y, Xu XW. 2016. Survival and growth of three afforestation species under high saline drip irrigation in the Taklimakan Desert, China. *Ecosphere.* 7(5):e01285.
- Zhu GF, Li X, Su YH, Lu L, Huang CL. 2011. Seasonal fluctuations and temperature dependence in photosynthetic parameters and stomatal conductance at the leaf scale of *Populus euphratica* Oliv. *Tree Physiol.* 31(2):178–195.